

# Cooperative and Active Sensing in Mobile Sensor Networks for Scalar Field Mapping

Hung M. La, *Member, IEEE*, Weihua Sheng, *Senior Member, IEEE*, and Jiming Chen, *Senior Member, IEEE*

**Abstract**—Scalar field mapping has many applications including environmental monitoring, search and rescue, etc. In such applications, there is a need to achieve a certain level of confidence regarding the estimates of the scalar field. In this paper, a cooperative and active sensing framework is developed to enable scalar field mapping using multiple mobile sensor nodes. The cooperative and active controller is designed via the real-time feedback of the sensing performance to steer the mobile sensors to new locations in order to improve the sensing quality. During the movement of the mobile sensors, the measurements from each sensor node and its neighbors are fused with the corresponding confidences using distributed consensus filters. As a result, an online map of the scalar field is built while achieving a certain level of confidence of the estimates. We conducted computer simulations to validate and evaluate our proposed algorithms.

**Index Terms**—Active sensing, cooperative sensing, flocking control, mobile sensor networks, sensor fusion.

## I. INTRODUCTION

### A. Motivation

IN recent years, measuring and exploring an unknown field of interest has attracted much attention of environmental scientists and control engineers [1]–[6]. Typical applications include environmental monitoring [7]–[12], mapping of oil spill or toxic-chemical pollution [13]–[16], etc. One example is the Gulf of Mexico oil spill in 2010. According to the National Oceanic and Atmospheric Administration (NOAA), an estimated 2 10 000 gallons a day leaked from the ruptures into the gulf [see Fig. 1(a)]. Another example is harmful algal bloom [see Fig. 1(b)] which can produce cyanotoxins [15] and has serious adverse health effects to humans and aquatic life as well [15], [16]. In order to tackle such pollution, it is desired

to build a map of the pollution field which may represent, for example, the density of the oil spill or the concentration of the algal bloom. Because the scalar field usually occupies a large area, MSNs offer an ideal solution to this mapping problem. To obtain an estimate of the scalar field, the sensor nodes need cooperate with each other in a distributed fashion.

In our previous work [17], [18], a cooperative sensing algorithm was developed for an MSN to build the map of the scalar field. Based on this algorithm, all mobile sensors can form a quasi-lattice formation and work together to estimate the value at each location of the field along with its own confidence of estimates. Since the cooperative controller is not active, the sensing performance or the confidence is not consistent over the field. This could negatively affect many scalar field mapping applications such as temperature field mapping, search, and rescue, where a need exists to achieve a certain level of confidence regarding the estimates at each location. Using the normal cooperative sensing algorithm developed in our previous papers [17], [18], we find that some locations (cells) have very low confidence. This means that the MSN may miss important information at these cells. For example, in search and rescue operations the MSN may miss the objects at the locations where the confidence of the estimate is low. Also, some cells may have very high confidence, which could cause unnecessary measurements and energy consumption. This motivates us to develop a new active sensing algorithm which can integrate both sensing and motion control to adapt to the environments so that the sensing performance can be improved.

There are several challenges that should be addressed. First, the active sensing algorithm should be designed in a distributed fashion so that each mobile sensor node only needs to cooperate with its neighbors to adjust its configurations. Second, the estimation and control have to be performed on-line in order to adapt to the changes of the environments. Third, the sensor fusion algorithm should also be designed in a distributed way to allow each sensor node to estimate the field in real time while only exchanging measurement information with its neighbors.

For simplicity, in this paper, we only focus on adjusting the relative location among sensor nodes while in other applications, the sensor configurations could include focal length, field of view of the cameras, etc. Specifically, our problem focuses on how to control the movement of the mobile sensors in a cooperative fashion to increase the confidence level of the estimates. We aim to ensure quasi-uniform confidence on the estimates. Here by quasi-uniform confidence we mean

Manuscript received June 28, 2013; revised December 8, 2013; accepted April 3, 2014. Date of publication May 14, 2014; date of current version December 12, 2014. This work was supported in part by the U.S. Department of Defense under DoD ARO DURIP Grant 55628-CS-RIP, in part by the DEPSCoR Grant W911NF-10-1-0015, in part by the NSF Grant CISE/IIS 1231671, in part by NSF-China Grant 61328302, in part by the Vietnamese Government under 322 project of the Ministry of Education and Training, and in part by NSF-China Grant 61222305, SKLICT Open project funding, NCET-11-0445. This paper was recommended by Associate Editor K. Hirota.

H. M. La is with the Department of Computer Science and Engineering, University of Nevada, Reno, NV 89557 USA (email: hung.m.la@ieee.org)

W. Sheng is with the School of Electrical and Computer Engineering, Oklahoma State University, Stillwater, OK 74078 USA (e-mail: weihua.sheng@okstate.edu).

J. Chen is with the State Key Laboratory of Industrial Control Technology, Department of Control, Zhejiang University, Hangzhou 310027, China (e-mail: jmchen@ieee.org).

Color versions of one or more of the figures in this paper are available online at <http://ieeexplore.ieee.org>.

Digital Object Identifier 10.1109/TSMC.2014.2318282

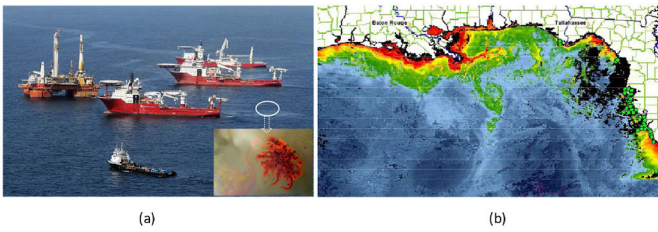


Fig. 1. (a) Oil spill in the Gulf of Mexico caused ships and rig workers to evacuate (Photo by Mario Tama/Getty Images). (b) Estimated field of chlorophyll generated by the harmful algal blooms observation system [16] by the National Oceanic and Atmospheric Administration (NOAA) (photo courtesy of NOAA).

that the confidence is within a lower and upper bound. In addition, our approach to sensor fusion is to use decentralized consensus filters and a weighted average update protocol to allow sensor nodes to quickly agree on the estimation.

In summary, the main contributions of this paper are as follows.

- 1) A distributed sensor fusion algorithm is developed for cooperative sensing and this algorithm integrates both spatial and temporal estimation based on consensus filters. A convergence analysis for the proposed distributed consensus filter is provided.
- 2) An active sensing algorithm is developed to incorporate the realtime feedback of sensing performance into the sensor motion control. Such a feedback control enables the mobile sensor network to achieve a quasi uniformity on the confidence of the estimates.
- 3) Simulation results are provided to verify the effectiveness of the proposed algorithms. Part of the work has been published in a conference paper [34].

## B. Literature Review

Cooperative sensing using MSNs has gained increasing interest in environmental modeling and coverage [1], [2], [6], [19], [35]. Cooperative sensing based on the gradient descent algorithms to obtain the optimal coverage is developed in [2], and optimal sensor placement for environment monitoring can be found in [35]. For dynamic environment coverage, a control strategy based on the discrete Kalman filter is developed [1]. The approach relies on the Kalman filter to estimate the field and on the filter's prediction step to plan the vehicles' next move to maximize the estimation quality. In [19], an optimal filtering approach to fusing local sensor data into a global model of the environment is developed. The approach is based on the use of average consensus filters to distributedly fuse the sensory data through the communication network. Along with the consensus filters, control laws are developed for mobile sensors to maximize their sensory information relative to current uncertainties in the model. Additionally, cooperative sensing algorithms have been developed for applications in environmental estimation [23], sampling and exploring [3], [4], [24]. More details of the existing works in this area can be seen in [36]. In [23], an MSN is deployed in an environment of interest, and takes measurements of a spatio-temporal random field. A distributed Kriged-Kalman filter is developed to

estimate the random field and its gradient. In [24], underwater vehicles are deployed to measure temperature and currents. The vehicles communicate via an acoustic local area network and coordinate their motion in response to local sensing information and evolving environments. This mobile sensor network aims to provide the ability to sample the environment adaptively in space and time. In [3], a class of underwater vehicles are used to obtain a sampling coverage over a large area via a cooperative control method. To further improve the cooperative sensing performance, both cooperative motion control and cooperative sensing are integrated based on a cooperative Kalman filter [4] to control the shape of the sensor node formation in order to minimize the estimation errors.

On the other hand, active sensing in MSNs has been studied by many researchers in control engineering [20]–[22], [25], [26], [33], [37], [38]. The early work can be found in [20] and [21] where an active sensing algorithm for MSNs to estimate the state of dynamic targets is proposed. To achieve active sensing, the mobility of sensing agents is utilized to improve the sensing performance. However, the gradient controller for active sensing is designed in a centralized way. To relax this limitation, a distributed gradient controller is proposed in [22]. This controller is designed by constructing a dynamic average consensus estimator and using a one-hop neighbor for communication so that both formation control and cooperative sensing are integrated to improve the sensing performance. Along with cooperative sensing, the active sensing algorithms for source seeking and radiation mapping have been developed [25]–[32]. The problem of source seeking is first addressed in [27], and then it is thoroughly studied in [28]–[30] for the case when direct gradient information of the measured quantity is unavailable. Specifically, Pang and Farrell [28] address chemical plume source localization by constructing a source likelihood map based on Bayesian inference methods. Mesquita *et al.* [29] introduce a source seeking behavior without direct gradient information by mimicking *E. coli* bacteria. Mayhew *et al.* [30] propose a hybrid control strategy to locate a radiation source utilizing only radiation intensity measurements. Additionally, active sensing for radiation mapping is developed in [25], [26]. The control algorithm takes into account sensing performance as well as dynamics of the observed process. Therefore, it can steer mobile sensors to locations where they maximize the information content of the measurement data.

The summary of related work is shown in Table I. All of the above mentioned cooperative and active sensing works mainly focus on target(s) tracking, sensor placement, source seeking, terrain reconstructions, and radiation mapping [10]. To the best of our knowledge, the problem of scalar field estimation and mapping based on multiagent cooperative and active sensing has not been fully addressed.

The rest of this paper is organized as follows. Section II first gives the details of the scalar field and measurement modeling and the problem formulation, then presents an overview of the approach to cooperative and active sensing for scalar field mapping using mobile sensor networks. Section III presents a distributed sensor fusion algorithm for mapping the unknown scalar field. Section IV proposes a design of the active

TABLE I  
SUMMARY OF RELATED WORK IN COOPERATIVE AND ACTIVE SENSING

Normal Cooperative Sensing (NCS)	Cooperative and Active Sensing (CAS)	CAS in Our paper
Environmental modeling and coverage [1], [2], [6], [19] Environment sampling and exploring [3], [4], [23], [24] Environment monitoring [12]	Target tracking [20]–[22] Radiation source seeking [25]–[32] Optimal sensor placement for target tracking [33]	Our paper presents a new approach for scalar field estimation and mapping using an MSN.
NCS is mainly designed based on Extended Kalman filter or Kriged Kalman filter, and no confidence feedback is used to allow the MSN to adjust its configuration to adapt the changes of the environments. Hence it is not suitable for the scalar field estimation and mapping.	CAS is mainly developed for target tracking and source seeking. Hence it is not appropriate to be applied in scalar field estimation and mapping problem.	This approach finds a quick agreement of estimations among sensor nodes using distributed consensus filters. Additionally, the active controller is designed to allow the MSN to adjust its configuration to adapt to the changes of the environments and improve the estimation confidence.

potential controller to improve the confidence performance. Section V shows the simulation results. Finally, Section VI concludes this paper.

## II. OVERVIEW

This section presents the problem statement of the cooperative and active sensing using a mobile sensor network for scalar field mapping, and then an overview of the approach to this problem.

### A. Problem Formulation

We first model a mobile sensor network as a dynamic graph  $G$  consisting of a vertex set  $\vartheta = \{1, 2, \dots, n\}$  and an edge set  $\zeta \subseteq \{(i, j): i, j \in \vartheta, j \neq i\}$ . In this graph, each vertex denotes a mobile sensor node, and each edge denotes the communication link between sensor nodes.

We then define a neighborhood set of sensor node  $i$  at time step  $t$  as follows:

$$N_i(t) = \{j \in \vartheta : \|q_j - q_i\| \leq r, \vartheta = \{1, 2, \dots, n\} j \neq i\} \quad (1)$$

here  $q_i \in R^2$  is the position of sensor node  $i$ ; and  $r$  is the communication (active) range of the sensor node.

We model the scalar field of interest in a 2-D space of  $(x, y)$  as [17]

$$F(x, y) = \Theta \Phi^T(x, y) = \sum_{j=1}^K \theta_j \phi_j(x, y) \quad (2)$$

here  $\Theta = [\theta_1, \theta_2, \dots, \theta_K]$ , and  $\Phi(x, y) = [\phi_1, \phi_2, \dots, \phi_K]$ , where  $\phi_j(x, y)$  is a function representing the density distribution, and  $\theta_j$  is the weight of the density distribution of the function  $\phi_j(x, y)$ .  $j$  is the index, and  $K$  is the total number of density distribution functions.

We partition the scalar field  $F$  into a grid of  $C$  cells. Each sensor  $i$  makes an observation (measurement) of the scalar field at cell  $k$  ( $k \in \{1, 2, \dots, C\}$ ) at time step  $t$

$$m_i^k(t) = O_i^k(t)[F^k(t) + n_i^k(t)] \quad (3)$$

here  $n_i^k(t)$  is uncorrelated noise with zero mean and variance  $V_i^k(t)$  at time step  $t$ , namely,  $n_i^k(t) \sim \mathcal{N}(0, V_i^k(t))$ .  $O_i^k(t)$  is the observability of sensor node  $i$  at cell  $k$  at time step  $t$ , and it is defined as

$$O_i^k(t) = \begin{cases} 1, & \text{if } \|q_i(t) - q_c^k\| \leq r_i^s \\ 0, & \text{otherwise} \end{cases} \quad (4)$$

where  $q_c^k \in R^2$  is the location of cell  $k$ ; and  $r_i^s$  is the sensing/measurement range of sensor node  $i$ .

Each mobile sensor node makes a measurement at cell  $k$  corresponding to its position. We assume that the variance  $V_i^k(t)$  is related to the distance between sensor node  $i$  and cell  $k$  according to

$$V_i^k(t) = \begin{cases} \frac{\|q_i(t) - q_c^k\|^2 + c_v}{(r_i^s)^2}, & \text{if } \|q_i(t) - q_c^k\| \leq r_i^s \\ 0, & \text{otherwise} \end{cases} \quad (5)$$

here  $0 < c_v < 1$ .

Given the measurements of the sensor node  $i$  in (3),  $m_i^k(t)$ , and its neighbors,  $m_j^k(t)$ , at each cell  $k$  of the scalar field  $F$  as modeled in (2) with observability  $O_i^k(t)$  in (4), and measurement variance  $V_i^k(t)$  in (5), our problem here is to design a distributed sensor fusion algorithm and an active control algorithm to allow mobile sensors to move together and build the map of the unknown scalar field, namely, the following.

- 1) Design consensus filters to allow each sensor node to find out the spatial estimation and the confidence of estimation of the field  $F$  at each cell  $k$ .
- 2) Design an online update protocol to allow each sensor node find out the final estimation and the confidence of estimation of the field  $F$  along the sensor movement.
- 3) Design an active and cooperative controller to allow the sensor nodes to form a network and actively adjust the configuration via feedback of sensing performance.

The constraints are as follows.

- 1) Each sensor only communicates with its neighbors to exchange the position information within its active range ( $r_i$ ).
- 2) Each sensor only communicates with its neighbors to exchange the measurement information within its sensing range ( $r_i^s$ ).
- 3) The confidence performance of the field estimation is maintained within a certain bound, or it should satisfy the quasi-uniform requirement.

### B. Overall Framework

This subsection presents a framework of cooperative and active sensing for scalar field mapping using mobile sensor networks. The sensors form a network and take measurements of the scalar field along their movement. These measurements are fused via the consensus filters and a weighted average protocol to obtain the estimates of the field. The confidence

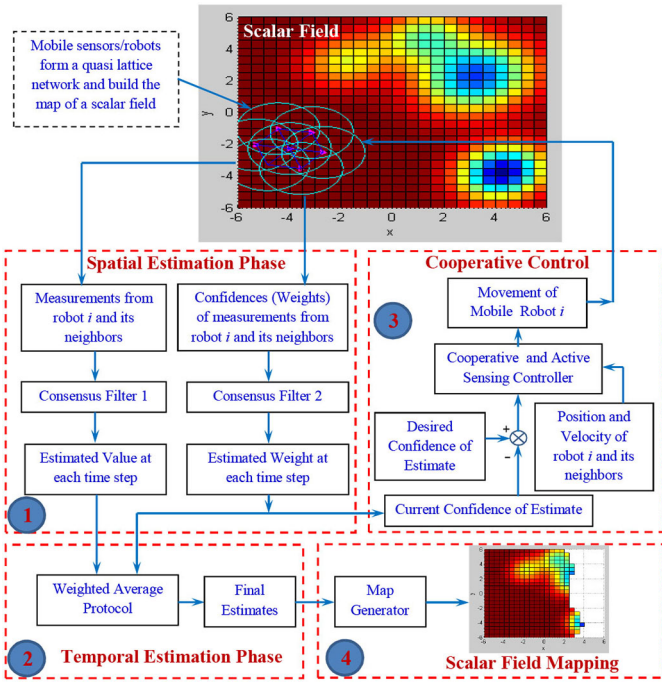


Fig. 2. Framework of the distributed sensor fusion algorithm and active sensing for scalar field mapping.

of the estimates is used as feedback for the controller to control the MSN to new locations to improve the sensing performance. The details of this active sensing framework are shown in Fig. 2.

The framework consists of four blocks 1–4. Block 1 (spatial estimation phase) and Block 2 (temporal estimation phase) represent the two update phases of the distributed sensor fusion algorithm. In the spatial estimation phase, the measurements of sensor node  $i$  and its neighbors at each cell are the inputs of Consensus Filter 1, which outputs the estimate of the value of the scalar field at each cell at each time step. The confidences (weights) of the measurements of each sensor node and its neighbors at each cell are the inputs of Consensus Filter 2, which outputs the estimate of the confidence. During the movement, each sensor node obtains a sequence of estimates of the value at each cell with associated confidence. These estimates and confidences will then be fused with a weighted average protocol to derive the final estimate in an iterative way.

Block 3 represents a cooperative and active controller which is designed based on the artificial potential field approach [39]–[41]. This controller only requires local information (position and velocity of each sensor node and its neighbors), but it can distributedly control the mobile sensors to first form a quasi-lattice network (see top of Fig. 2) and then move the MSN in the desired trajectory to cover the whole scalar field. Based on the real-time feedback of the confidence of estimates the active controller can allow the mobile sensors to move to locations which have a low level of confidence and steer away locations which have a high level of confidence to achieve better sensing performance.

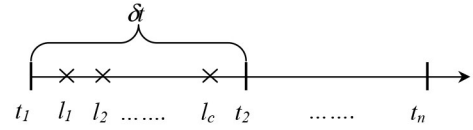


Fig. 3. Illustration of the relation between iteration index  $l$  and time step  $t$ .

Block 4 represents scalar field mapping. The final estimate at each cell of the scalar field obtained from the temporal estimation phase goes to the map generator, and then the map of the field is created online corresponding to the location of the MSN.

### III. DISTRIBUTED SENSOR FUSION ALGORITHM

This section presents a distributed sensor fusion algorithm which consists of two consensus filters which allow each sensor to exchange the information among its neighbors, and the average update protocol which allows each sensor to update the final estimation of the scalar field at each cell.

#### A. Consensus Filter 1

Since each sensor may have different measurements to the cell  $k$  of the scalar field  $F$ , the Consensus Filter 1 is introduced to find the agreement among these measurements.

Let  $x_i^k(l)$  be the spatial measurement of sensor node  $i$  at cell  $k$ , and the initial condition for this measurement state is given as  $x_i^k(l=0) = m_i^k(t)$  as defined in (3). Similar to [42]–[44], we have distributed linear iterations of the following form:

$$x_i^k(l+1) = w_{ii}^k(t)x_i^k(l) + \sum_{j \in N_i(t)} w_{ij}^k(t)x_j^k(l) \quad (6)$$

here  $l$  is the iteration index in the running process of the consensus filter, and  $t$  is time step (see Fig. 3) at which sensor  $i$  makes an observation/measurement to cell  $k$ . Specifically, at each time step  $t$  sensor  $i$  runs the consensus filter (6). We assume that  $\delta t = t(k) - t(k-1)$  is large enough so that after several iterations the consensus filter can find an agreement among all measurements of sensors by exchanging information with its neighbors. The weight,  $w_{ii}^k(t)$ , is the self weight or vertex weight of each sensor to cell  $k$ , and  $w_{ij}^k(t)$  is the edge weight between sensor  $i$  and sensor  $j$ . These weights are defined as follows [17]:

$$w_{ij}^k(t) = \begin{cases} \frac{c_1^w}{V_i^k(t)}, & (V_i^k(t) \neq 0), & \text{if } i = j \\ \frac{1-w_{ii}^k(t)}{|N_i(t)|}, & & \text{if } i \neq j, j \in N_i(t) \\ 0, & & \text{otherwise} \end{cases} \quad (7)$$

here,  $c_1^w$  is constant and satisfies the following condition [17]:

$$0 < c_1^w < \frac{c_v}{(r_i^s)^2}. \quad (8)$$

The convergence of Consensus Filter 1 is given in the Appendix. For more details of this consensus design please refer to [17].

### B. Consensus Filter 2

Different to the Consensus Filter 1 which is used to find the agreement among the measurements of the sensor nodes, the Consensus Filter 2 is introduced to find the agreement of the confidences of spatial measurements of sensor nodes.

Let  $y_i^k(l)$  be the spatial confidence of the measurement of sensor node  $i$  at cell  $k$ , and the initial condition for this confidence state is given as  $y_i^k(l=0) = w_{ii}^k(t)$  as defined in (7). Then, we have the following consensus filter:

$$y_i^k(l+1) = M_{ii}^k(t)y_i^k(l) + \sum_{j \in N_i(t)} M_{ij}^k(t)y_j^k(l) \quad (9)$$

here  $M_{ij}^k(t)$  is the Metropolis weight [42] as

$$M_{ij}^k(t) = \begin{cases} \frac{1}{1 + \max(|N_i(t)|, |N_j(t)|)}, & \text{if } i \neq j, j \in N_i(t) \\ 1 - \sum_{j \in N_i(t)} M_{ij}^k(t), & \text{if } i = j \\ 0, & \text{otherwise} \end{cases} \quad (10)$$

When Consensus Filter 2 converges, it will give the overall confidence of the estimate at cell  $k$ . We call this overall confidence as the estimated weight,  $W_i^k(t)$ , and this weight will be used in the temporal estimation phase.

### C. Average Update Protocol

Let  $l_c$  be an iteration that both consensus filters 1 and 2 converge (see Fig. 3), then we can obtain the value estimate  $E_i^k(t)$  of cell  $k$  associated with the estimated weight  $W_i^k(t)$  as follows:

$$\begin{cases} E_i^k(t) = x_i^k(l_c) \\ W_i^k(t) = y_i^k(l_c). \end{cases} \quad (11)$$

From the result of estimates in (11) we can find the final estimate of the value of the scalar field at each cell  $k$  via the following process.

- 1) Update weight/confidence

$$\bar{W}_i^k(t) = W_i^k(t-1) + W_i^k(t-2) + \dots + W_i^k(0). \quad (12)$$

- 2) Update the final estimate based on the Weighted Average protocol

$$\bar{E}_i^k(t=0) = E_i^k(t=0) = x_i^k(l_c) \quad (13)$$

$$\bar{E}_i^k(t) = \frac{\bar{W}_i^k(t-1)\bar{E}_i^k(t-1) + W_i^k(t)E_i^k(t)}{\bar{W}_i^k(t-1) + W_i^k(t)}. \quad (14)$$

## IV. POTENTIAL CONTROLLER DESIGN FOR ACTIVE SENSING

In this section we aim to develop a potential controller for cooperative and active sensing, and the main idea of our approach is shown in Block 3 in Fig. 2. Our purpose is to use the feedback of the estimation confidence to adjust the movement of the sensors so that they can improve the sensing performance in a distributed fashion. Specifically, the potential controller is designed to steer the mobile sensors to the new locations in order to achieve the quasi uniformity of the confidence. First, we describe the flocking control algorithm [45], [46] for mobile sensors to move together.

We consider  $n$  mobile sensor nodes moving in a 2-D Euclidean space. The dynamic equations of each sensor node are described as

$$\begin{cases} \dot{q}_i = p_i \\ \dot{p}_i = u_i, \quad i = 1, 2, \dots, n \end{cases} \quad (15)$$

here  $q_i$  and  $p_i \in R^2$  are the position and velocity of sensor node  $i$ , respectively, and  $u_i$  is the control input of sensor node  $i$ .

The geometry of the MSN is modeled by an  $\alpha$ -lattice [45] that meets the following condition:

$$\|q_j - q_i\| = d, j \in N_i(t) \quad (16)$$

here  $d$  is a positive constant indicating the distance between sensor node  $i$  and its neighbor  $j$ . However, at singular configuration ( $q_i = q_j$ ) the collective potential used to construct the geometry of flocks is not differentiable. Therefore, the set of algebraic constraints in (16) is rewritten in term of  $\sigma$ -norm [45] as follows:

$$\|q_j - q_i\|_\sigma = d^\alpha, \quad j \in N_i(t) \quad (17)$$

here the constraint  $d^\alpha = \|d\|_\sigma$  with  $d = r/k_c$ , where  $k_c$  is the scaling factor. The  $\sigma$ -norm,  $\|\cdot\|_\sigma$ , of a vector is a map  $R^m \implies R_+$  defined as  $\|z\|_\sigma = \frac{1}{\epsilon}[\sqrt{1 + \epsilon\|z\|^2} - 1]$  with  $\epsilon > 0$ . Unlike the Euclidean norm  $\|z\|$ , which is not differentiable at  $z = 0$ , the  $\sigma$ -norm  $\|z\|_\sigma$ , is differentiable everywhere.

The flocking control algorithm which consists of the formation control term and the leader tracking control term is represented as

$$u_i = f_i^\alpha + f_i^t. \quad (18)$$

The formation controller [45] is used to control the network to form a quasi-lattice formation, and it is designed based on a pairwise attractive/repulsive force

$$f_i^\alpha = c_1^\alpha \sum_{j \in N_i} \phi_\alpha(\|q_j - q_i\|_\sigma) n_{ij} + c_2^\alpha \sum_{j \in N_i} a_{ij}(q)(p_j - p_i) \quad (19)$$

where  $c_1^\alpha$  and  $c_2^\alpha$  are positive constants,  $\phi_\alpha(z)$  is the action function,  $n_{ij}$  is the vector along the line connecting  $q_i$  to  $q_j$ , and  $[a_{ij}(q)]$  is the adjacency matrix. For more detail of these terms, please refer to [45].

The leader tracking controller is used to control each mobile sensor to track the virtual leader. The trajectory of the virtual leader is planned so that the MSN can cover the entire scalar field. This controller is presented as

$$f_i^t = -c_1^t(q_i - q_t) - c_2^t(p_i - p_t) \quad (20)$$

here  $c_1^t$  and  $c_2^t$  are positive constant, and  $q_t$  and  $p_t$  are position and velocity of the virtual leader, respectively.

### A. Design of Attractive Force

In this subsection, we introduce the attractive force term to the flocking controller (18) to increase the confidence level of estimates over the lower bound. The attractive force will steer the mobile sensors to the cells which have low confidence. In order to do this, first let  $q_c^k$  be the location of the cell that

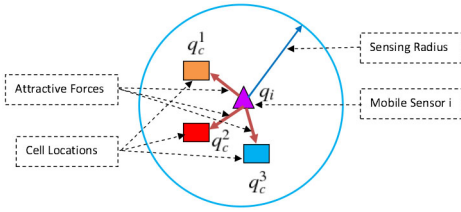


Fig. 4. Creating virtual attractive forces in the cells which have confidence level lower than the lower bound.

---

**Algorithm 1: Design of Attractive Force**


---

**if**  $O_i^L(t) \neq \emptyset$  **or**  $\Delta_W^k(t) > 0$  **then**

$$f_i^{\text{att}} = - \sum_{k \in O_i^L(t)} C_k^{\text{att}} \phi_{\text{att}}(\|q_c^k - q_i\|_{\sigma}) n_{i,k}^{\text{att}}$$

$$C_k^{\text{att}} = c_a \frac{\Delta_W^k(t)}{\sqrt{1 + (\Delta_W^k(t))^2}}, \Delta_W^k(t) \in \Delta_W^L(t), \text{ here } c_a \text{ is a positive constant.}$$

**else**

$$f_i^{\text{att}} = 0 \quad (22)$$

**end**

---

has confidence lower than the lower bound, or  $k \in O_i^L(t)$ , here  $O_i^L(t)$  is the subset of cells covered by mobile sensor  $i$  at time  $t$ , which have confidence lower than the lower bound.  $O_i^L(t) \subset O_i^c(t)$ , here  $O_i^c(t)$  is the set of cells covered by mobile sensor  $i$  at time  $t$ , and it is defined as

$$O_i^c(t) = \left\{ k \in \mathcal{O}: \|q_c^k - q_i\| \leq r_i^s, \mathcal{O} = \{1, 2, \dots, k\} \right\}. \quad (21)$$

For these cells we will create the virtual attractive force to attract the mobile sensor to move closer to them in order to get higher confidence of the estimates at these cells. This idea is illustrated in Fig. 4.

At each time  $t$ , the mobile sensor  $i$  may have several cells which have confidence lower than the desired one. In order to steer the mobile sensor to go to these low confidence cells, the virtual attractive forces are generated at these cells. If the cell has lower confidence a bigger attractive force is generated.

Let  $\bar{W}_d^L$  be the lower bound of the desired confidence of the estimates of all cells in the scalar field.  $\bar{W}_d^L$  is a vector of  $1 \times C$  dimension. Let  $\Delta_W^L(t) = \bar{W}_d^L - \bar{W}(t)$  be the difference between the current confidence and the lower bound (see Fig. 5),  $\Delta_W^L(t) = [\Delta_W^1(t), \Delta_W^2(t), \dots, \Delta_W^C(t)]$ . Based on this feedback,  $\Delta_W^L(t)$ , we can design an attractive force as shown in Algorithm 1.

In Algorithm 1,

$$C_k^{\text{att}} = c_a \frac{\Delta_W^k(t)}{\sqrt{1 + (\Delta_W^k(t))^2}}$$

controls the magnitude of the attractive force. Namely, if cell  $k$  has low confidence or  $\Delta_W^k(t)$  is large, the the magnitude of the attractive force is big in order to attract the mobile sensor to get closer this cell.

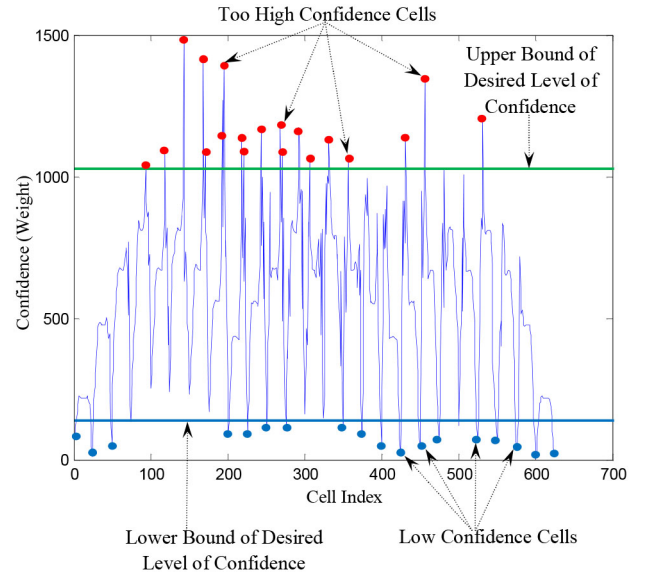


Fig. 5. Illustration of confidence feedback for quasi uniformity of the confidence. The upper bound and lower bound are used to create a quasi uniform of the confidence. The confidences of the estimates are obtained using the cooperative flocking controller in our previous work [17].

The attractive force function  $\phi_{\text{att}}(\|q_c^k - q_i\|_{\sigma})$  is designed as

$$\phi_{\text{att}}(\|q_c^k - q_i\|_{\sigma}) = \rho_h \left( \frac{\|q_c^k - q_i\|_{\sigma}}{r_{\alpha}^s} \right) \frac{\|q_c^k - q_i\|_{\sigma}}{\sqrt{1 + \|q_c^k - q_i\|_{\sigma}^2}} \quad k \in O_i^L(t)$$

here,  $r_{\alpha}^s = \|r^s\|_{\sigma}$  ( $r^s$  is the sensing range as defined before), and similar to [45] the bump function  $\rho_h \left( \frac{\|q_c^k - q_i\|_{\sigma}}{r_{\alpha}^s} \right)$  with  $h \in (0, 1)$  is defined as

$$\rho_h \left( \frac{\|q_c^k - q_i\|_{\sigma}}{r_{\alpha}^s} \right) = \begin{cases} 1, & \text{if } \frac{\|q_c^k - q_i\|_{\sigma}}{r_{\alpha}^s} \in [0, h) \\ 0.5 \left[ 1 + \cos \left( \pi \left( \frac{\frac{\|q_c^k - q_i\|_{\sigma}}{r_{\alpha}^s} - h}{1-h} \right) \right) \right], & \text{if } \frac{\|q_c^k - q_i\|_{\sigma}}{r_{\alpha}^s} \in [h, 1] \\ 0, & \text{otherwise.} \end{cases} \quad (23)$$

The vector along the line connecting  $q_c^k$  ( $k \in O_i^L(t)$ ) and  $q_i$  is defined as

$$n_{ik}^{\text{att}} = (q_c^k - q_i) / \sqrt{1 + \epsilon \|q_c^k - q_i\|^2}, \quad k \in O_i^L(t) \quad (24)$$

here,  $\epsilon$  is a small positive constant.

The control algorithm for the cooperative and active sensing including the attractive force term only is presented as

$$\begin{aligned} u_i &= f_i^{\text{att}} + f_i^{\alpha} + f_i^t \\ &= \sum_{k \in O_i^L(t)} C_k^{\text{att}} \phi_{\text{att}}(\|q_c^k - q_i\|_{\sigma}) n_{i,k}^{\text{att}} \\ &\quad + c_1^{\alpha} \sum_{j \in N_i(t)} \phi_{\alpha}(\|q_j - q_i\|_{\sigma}) n_{ij} \\ &\quad + c_2^{\alpha} \sum_{j \in N_i(t)} a_{ij}(q)(p_j - p_i) \\ &\quad - c_1^t (q_i - q_t) - c_2^t (p_i - p_t) \end{aligned} \quad (25)$$

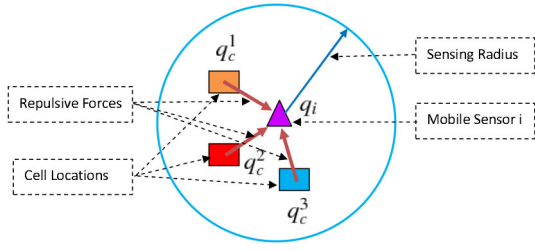


Fig. 6. Creating virtual repulsive forces in the cells which have confidence level higher than the upper bound.

---

**Algorithm 2: Design of Repulsive Force**


---

```

if  $O_i^H(t) \neq \emptyset$  or  $\Delta_W^k(t) < 0$  then
     $f_i^{\text{rep}} = \sum_{k \in O_i^H(t)} C_k^{\text{rep}} \phi_{\text{rep}}(\|q_c^k - q_i\|_\sigma) n_{i,k}^{\text{rep}}$ 
     $C_k^{\text{rep}} = c_r \frac{|\Delta_W^k(t)|}{\sqrt{1 + (\Delta_W^k(t))^2}}$ ,  $\Delta_W^k(t) \in \Delta_W^H(t)$ , here  $c_r$  is a
    positive constance.
else
     $f_i^{\text{rep}} = 0$ 
end

```

---

### B. Quasi Uniformity of Confidence

Based on the attractive force design in the previous subsection, the confidence level can be increased. However, some cells may have very high confidence, which will cause unnecessarily measurements and energy consumption. Therefore, it is desirable if we can maintain both lower and upper bounds of the confidence performance, or we call a quasi-uniform confidence (see Fig. 5). Hence, we introduce a repulsive force term to the flocking controller (18) in order to steer the mobile sensors to move away from the cells which have high confidence. The main idea of this design is to create a virtual attractive force at the cells that have lower confidence than the lower bound, and a repulsive force at the cells that have higher confidence than the upper bound (see Fig. 5).

Let  $q_c^k$  be the location of the cell that has confidence higher than the upper bound (see Fig. 5). For these cells we will create the virtual repulsive force to steer the mobile sensors to move away. This idea is illustrated in Fig. 6. The repulsive force is created based on the  $f_i^{\text{rep}}$  controller as shown in Algorithm 2.

Let  $\bar{W}_d^H$  be the upper bound of the desired confidence, and  $\bar{W}_d^H$  is a vector of  $1 \times C$  dimension. Let  $\Delta_W^H(t) = \bar{W}_d^H - \bar{W}(t)$  be the difference between the current confidence and the upper bound,  $\Delta_W^H(t) = [\Delta_W^1(t), \Delta_W^2(t), \dots, \Delta_W^C(t)]$ . Based on this feedback,  $\Delta_W^H(t)$ , we can design a repulsive force as shown in Algorithm 2.

In this algorithm,  $O_i^H(t)$  is the subset of cells covered by mobile sensor  $i$  at time  $t$ , which have confidence higher than the upper bound. Obviously,  $O_i^H(t) \subset O_i^c(t)$ .  $C_k^{\text{rep}}$  is used to control the magnitude of the repulsive force. Namely, if cell  $k$  has high confidence, or  $\Delta_W^k(t)$  is large, the magnitude of the

repulsive force is big in order to push the mobile sensor to move away from this cell.

The repulsive force function  $\phi_{\text{rep}}(\|q_c^k - q_i\|_\sigma)$  is designed as

$$\begin{aligned} \phi_{\text{rep}}(\|q_c^k - q_i\|_\sigma) &= \rho_h \left( \frac{\|q_c^k - q_i\|_\sigma}{r_\alpha^s} \right) \\ &\times \left( \frac{\|q_c^k - q_i\|_\sigma - r_\alpha^s}{\sqrt{1 + (\|q_c^k - q_i\|_\sigma - r_\alpha^s)^2}} - 1 \right) \\ &k \in O_i^H(t). \end{aligned}$$

The bump function  $\rho_h(\frac{\|q_c^k - q_i\|_\sigma}{r_\alpha^s})$  is defined as (23), but it is now applied for the high confidence cells or  $k \in O_i^H(t)$ . The vector along the line connecting  $q_c^k$  ( $k \in O_i^H(t)$ ) and  $q_i$  is defined as

$$n_{ik}^{\text{rep}} = (q_c^k - q_i) / \sqrt{1 + \epsilon \|q_c^k - q_i\|^2}, k \in O_i^H(t). \quad (27)$$

The whole control algorithm for the cooperative and active sensing including both attractive and repulsive force terms is presented as follows:

$$\begin{aligned} u_i &= f_i^{\text{rep}} + f_i^{\text{att}} + f_i^\alpha + f_i^t \\ &= \sum_{k \in O_i^H(t)} C_k^{\text{rep}} \phi_{\text{rep}}(\|q_c^k - q_i\|_\sigma) n_{i,k}^{\text{rep}} \\ &\quad + \sum_{k \in O_i^L(t)} C_k^{\text{att}} \phi_{\text{att}}(\|q_c^k - q_i\|_\sigma) n_{i,k}^{\text{att}} \\ &\quad + c_1^\alpha \sum_{j \in N_i(t)} \phi_\alpha(\|q_j - q_i\|_\sigma) n_{ij} \\ &\quad + c_2^\alpha \sum_{j \in N_i(t)} a_{ij}(q)(p_j - p_i) \\ &\quad - c_1^t (q_i - q_t) - c_2^t (p_i - p_t). \end{aligned} \quad (28)$$

## V. SIMULATION RESULTS

In this section, we test the cooperative and active sensing algorithm and compare it with the normal cooperative sensing algorithm [17], [18] in terms of sensing performance.

### A. Scalar Field Mapping with Cooperative and Active Sensing Algorithm

We model the environment (scalar field  $F$ ) as multiple variate Gaussian distributions. The scalar vector  $\Theta$  can be arbitrarily selected, for example  $\Theta = [20 \ 50 \ 35 \ 40]$ , corresponding to four multiple variate Gaussian distributions ( $K = 4$ ),  $\phi_1, \phi_2, \phi_3, \phi_4$ , and each one is represented as

$$\phi_1 = \frac{1}{\sqrt{\det(C_1)(2\pi)^2}} e^{-\frac{1}{2}(x-2)C_1^{-1}(y-2)^T}$$

here  $C_1 = \begin{bmatrix} 2.25 & 0.2999 \\ 0.2999 & 2.25 \end{bmatrix}$ , with the correlation factor  $c_1^0 = 0.1333$ .

For the functions  $\phi_2, \phi_3, \phi_4$ : the means  $(\mu_x, \mu_y)$  are  $(1, 0.5)$ ,  $(4.3, 3.5)$ ,  $(3, -3)$ , respectively; the matrix  $C_2 = C_3 = C_4 = \begin{bmatrix} 1.25 & 0.1666 \\ 0.1666 & 1.25 \end{bmatrix}$ ; the correlation factor  $c_4^0 = c_3^0 = c_2^0 = c_1^0$ . We set the lower bound of the confidence level to be  $0.5 \times 10^5$ , and the higher bound of the confidence level to be  $1.9 \times 10^5$ .

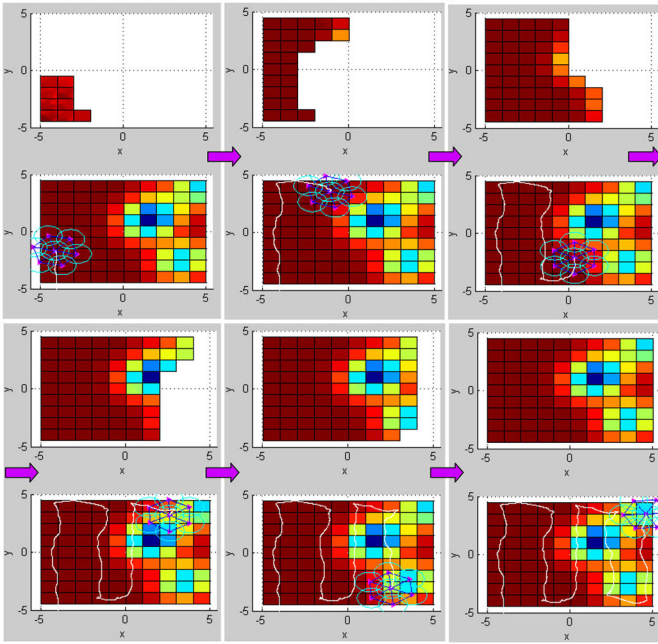


Fig. 7. Snapshots of building the map of the scalar field  $F$  using the active Potential Controller (28).

1) *Parameters of the cooperative and active control algorithm (28)*: Number of sensors = 7; the communication range  $r = k_c * d$  with  $d = 1.38$  and  $k_c = 1.2$ ;  $\epsilon = 0.1$  for the  $\sigma$ -norm;  $h = 0.2$  for the bump functions which are used to compute functions  $\phi_{att}(z)$  and  $\phi_{rep}(z)$ . To compute  $f_i^\alpha$ , parameters  $c_1^\alpha = 141$  and  $c_2^\alpha = 2 * \sqrt{c_1^\alpha}$ . The sensing range for each sensor node  $r_i^s = r - 0.6$ . Other parameters:  $c_a = 10$  and  $c_r = 190$ .

2) *Parameters for coverage path planning*: To compute  $f_i^t$ , parameters  $c_1^t = 25$  and  $c_2^t = 2 * \sqrt{c_1^t}$ . The virtual leader is planned to move in the predefined trajectory so that MSN can follow and cover the entire field. Namely, the step size  $\Delta_t = 0.008$ , and  $q_t = [-4, -6 + t]^T$  with  $0 \leq t \leq 10.5$ ;  $q_t = [-14.5 + t, 4.5]^T$  with  $10.5 \leq t < 12.5$ ;  $q_t = [-2, 17 - t]^T$  with  $12.5 \leq t < 21$ ;  $q_t = [-23 + t, -4]^T$  with  $21 \leq t < 23$ ;  $q_t = [0, -27 + t]^T$  with  $23 \leq t < 31.5$ ;  $q_t = [-31.5 + t, 4.5]^T$  with  $31.5 \leq t < 33.5$ ;  $q_t = [2, 38 - t]^T$  with  $33.5 \leq t < 42$ ;  $q_t = [-40 + t, -4]^T$  with  $42 \leq t < 44.5$ ; and  $q_t = [4.5, -48 + t]^T$  with  $44.5 \leq t \leq 54.5$ .

The snapshots of multiple sensor nodes forming a flock and building the map of the unknown scalar field are shown in Fig. 7. Fig. 8(a) shows the confidence of the estimates over cells, and (b) shows the map error corresponding to the index of the cell. We can see that the higher confidence corresponds to the smaller errors, and the lower confidence may lead to bigger errors. More specifically, at the 10th, 92th, and 100th cells, the confidences are the smallest, therefore at these cells the errors between the original map and the built map are the biggest.

The whole program is written in MATLAB and run on a Sony Vaio laptop which has a Core i3 Chip and 4GB RAM. The total running time for the MSN to build the entire scalar field map is 5 min and 590 s.

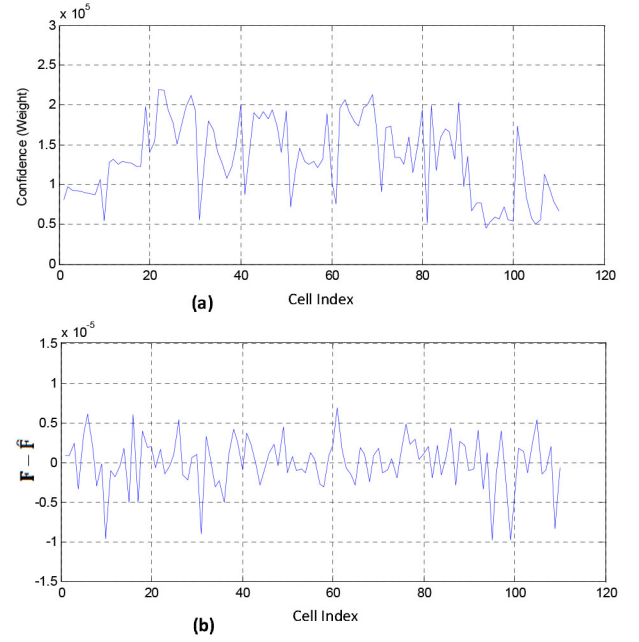


Fig. 8. (a) Confidence over cells. (b) Error between the original map and the built map in one dimension over cells.

### B. Different Initial Deployment Evaluation

To further evaluate the proposed cooperative and active sensing algorithm, different testing scenarios with different initial locations of sensor nodes and different path planings of the MSN are performed. The results are shown in Fig. 9. In Case 1 and 2 [Fig. 9(a) and (b)], different initial sensor locations are compared. In Case 3 [Fig. 9(c)], different coverage path planning of the MSN is compared. The results of these comparisons are shown in Fig. 9(d)–(f). We can see that the results of the map estimation confidence performance, the number of measurements over cells, and the map error in these three testing cases are similar. This tells that even with different deployment of location and path planning coverage of the MSN, the map estimation performance is similar.

### C. Algorithm Comparisons

In this subsection, we compare the cooperative and active sensing algorithm in both cases: the Potential Controller with attractive force only (25); and the Potential Controller with both attractive and repulsive forces (28). Then we compare it with the normal cooperative sensing algorithm in [17] and [18].

The confidence maps in 2-D created by Potential Controllers are shown in Fig. 10. This 2-D confidence map shows the confidence of the estimate at each cell corresponding to its location in the scalar field. We can see that the Potential Controller using both attractive and repulsive forces performs better than that of using only the attractive force since the confidence level is increased, and the quasi uniformity of the confidence performance is achieved.

The final confidence of the estimate in one dimension at each cell of the field  $F$  is shown in Fig. 11. In this figure we compared three methods. Namely, Fig. 11(a)

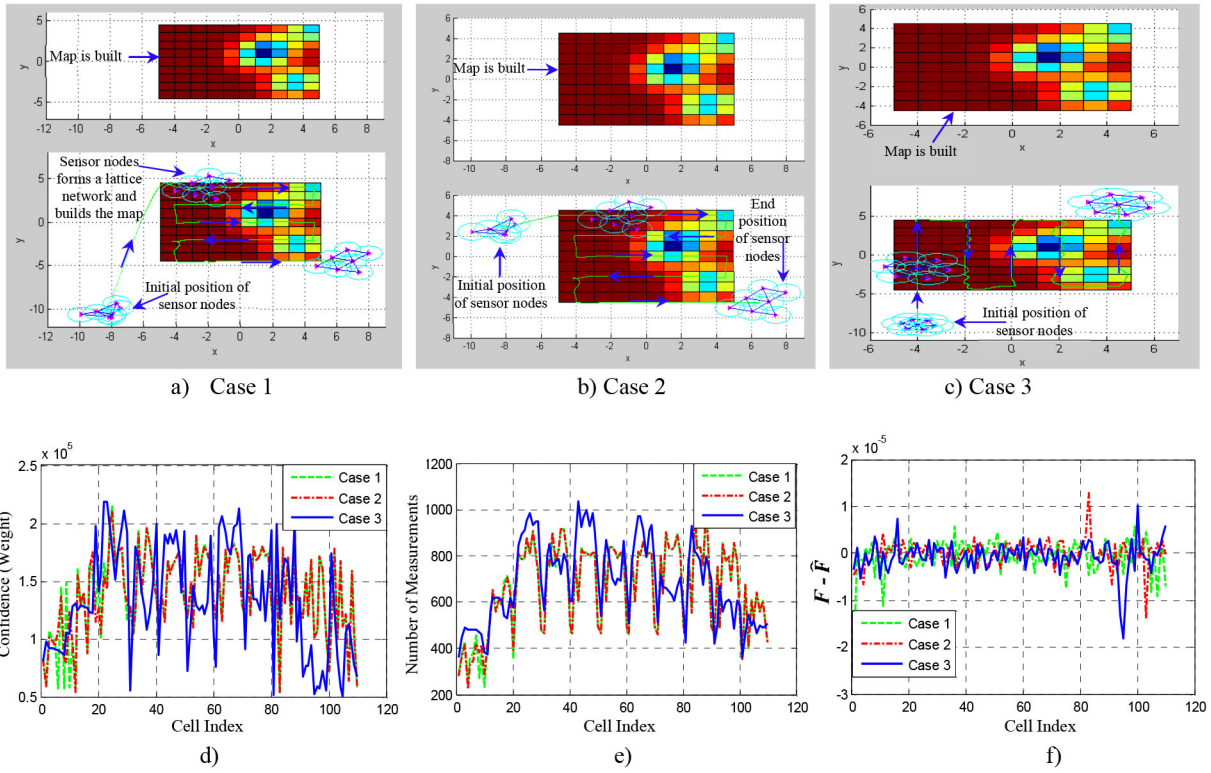


Fig. 9. (a)–(c) Different testing scenarios with different initial locations of sensor nodes and different path planning of the MSN are compared. (d) Confidence performance comparison for Cases 1, 2, 3. (e) Number of Measurement comparison for Cases 1, 2, 3. (f) Map error comparison for Cases 1, 2, 3.

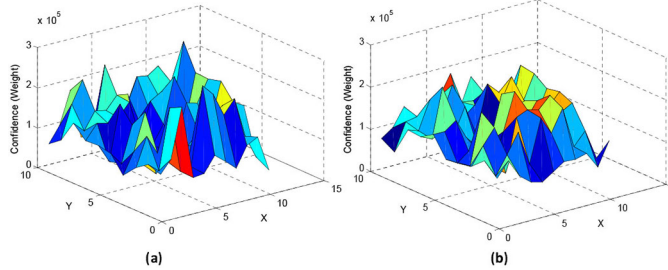


Fig. 10. Confidence over the cells in 2-D. (a) For active sensing with Potential Controller using attractive force only (25). (b) For active sensing with Potential Controller using both attractive and repulsive forces (28).

shows the confidence of the Potential Controller without attractive and repulsive forces. Fig. 11(b) shows the confidence of the Potential Controller with attractive force only. Fig. 11(c) shows the confidence of the Potential Controller with both attractive and repulsive forces. From these results, we can see that by using both attractive and repulsive force controllers we have better uniformity of the confidence performance.

To show the advantages of the active sensing we compare it with the normal sensing [17], [18] in term of mapping error as shown in Fig. 12. We can see that the error between the original map and the built map over cells is smaller when applying the active sensing, compared to that when applying the normal sensing.

To see the effectiveness of the quasi uniformity of the confidence, we collect the total number of measurements at each

cell in both cases of the active sensing algorithm as shown in Fig. 13. We can see that for the active sensing algorithm using attractive force only, some cells have very high number of measurements. For the active sensing algorithm using both attractive and repulsive forces, the number of measurements at these cells are reduced while the sensing performance (map error) is maintained.

## VI. CONCLUSION

This paper presented a cooperative and active sensing framework for mobile sensor networks to build the map of an unknown scalar field. Based on the proposed cooperative and active sensing controller, the mobile sensors can form a quasi-lattice network and automatically adjust their movement to achieve quasi-uniform confidence through a potential field based feedback control algorithm. The sensor fusion algorithm constructed by both spatial and temporal update phases allows the mobile sensors to collect and fuse the noisy measurements distributedly and simultaneously. The proposed cooperative and active sensing framework overperforms the normal cooperative sensing in term of sensing performance. Simulation results are collected to demonstrate the proposed algorithms.

In the future, we plan to implement our proposed algorithm on real mobile sensor networks. Additionally, we would like to investigate how to change other sensor configurations of the mobile sensor networks. For example, we can change the orientation and focal length of cameras, if they are used as the mobile sensors.

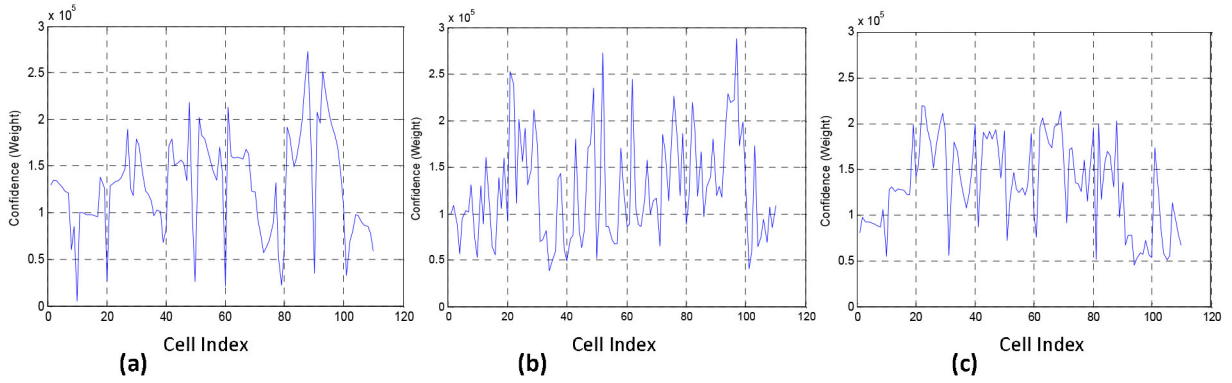


Fig. 11. Confidence over the cells in one dimension. (a) For normal cooperative sensing with the flocking controller (18). (b) For active sensing with Potential Controller using only attractive force (25). (c) For active sensing with Potential Controller using both attractive and repulsive forces (28).

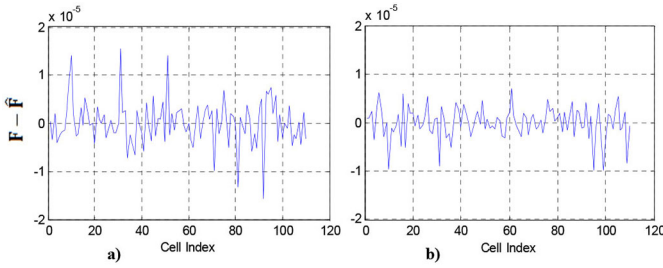


Fig. 12. Error between the original map and the built map in one dimension over cells. (a) For the normal sensing with the flocking controller (18). (b) For the active sensing (28).

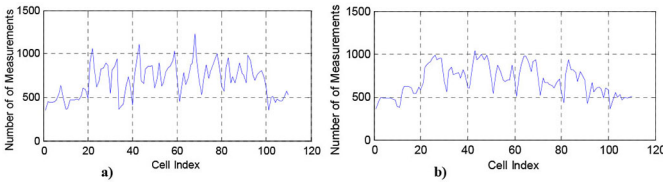


Fig. 13. Total number of measurements at each cell. (a) For Potential Controller with attractive force only (25). (b) For Potential Controller with both attractive and repulsive force (28).

## APPENDIX

In this Appendix, we analyze the convergence of the Consensus Filter 1.

First, let us define the weight matrix for the whole network as

$$\mathbf{w}^k = \begin{bmatrix} w_{11}^k & w_{12}^k & \cdots & w_{1n}^k \\ w_{21}^k & w_{22}^k & \cdots & w_{2n}^k \\ \vdots & \vdots & \cdots & \vdots \\ \vdots & \vdots & \cdots & \vdots \\ w_{n1}^k & w_{n2}^k & \cdots & w_{nn}^k \end{bmatrix}_{n \times n}. \quad (29)$$

Based on our weight design in (7), the matrix  $\mathbf{w}^k$  has the following properties.

(P1)  $w_{ij}^k = 0$  if  $j \notin N_i$ .

(P2) All elements,  $w_{ij}^k$ ,  $i = 1, \dots, n$  and  $j \in N_i$ , of the matrix  $\mathbf{w}^k$  satisfy  $0 < w_{ij}^k < 1$ .

(P3) Sum of all elements in each row of the matrix  $\mathbf{w}^k$  equals to 1.

With the definition of the weight matrix  $\mathbf{w}^k$ , we can expand (6) to  $n$  mobile sensors into space representation as follows:

$$\mathbf{x}^k(l+1) = \mathbf{w}^k \mathbf{x}^k(l) \quad (30)$$

or we have

$$\mathbf{x}^k(l+1) - \mathbf{x}^k(l) = [\mathbf{w}^k - \mathbf{I}] \mathbf{x}^k(l) \quad (31)$$

here  $\mathbf{I}$  is the identity matrix.

Let  $\Delta \mathbf{x}^k = \mathbf{x}^k(l+1) - \mathbf{x}^k(l)$ , from (31) we have

$$\Delta \mathbf{x}^k = [\mathbf{w}^k - \mathbf{I}] \mathbf{x}^k(l). \quad (32)$$

We can rewrite (32) into a continuous fashion

$$\dot{\mathbf{x}}^k = \mathbf{A}^k \mathbf{x}^k \quad (33)$$

here  $\mathbf{A}^k = \mathbf{w}^k - \mathbf{I}$ .

*Theorem 1:* Given any connected network, and by applying the Consensus Filter 1 as defined in (6) associated with the weight design as defined in (7), the system (33) is stable, or  $\Delta \mathbf{x}^k$  converges to zero.

*Proof:* The system (33) is a linear time-invariant system or autonomous system. Therefore, to show this system is stable we need to show that matrix  $\mathbf{A}^k$  is Hurwitz, or all of the roots of the characteristic equation have negative real parts [47].

Given a matrix  $B = [b_{ij}]_{n \times n}$  of the autonomous system  $\dot{\mathbf{x}} = B\mathbf{x}$  we have the following theorem.

*Theorem 2 (Liao et al. [48]):* If the following conditions: (C1)  $b_{ii} < 0$  ( $i = 1, 2, \dots, n$ ) and  $\det(B) \neq 0$ ; and (C2) there exist constants  $c_i > 0$  ( $i = 1, 2, \dots, n$ ) such that  $c_j b_{ij} + \sum_{i=1, i \neq j}^n |c_i| |b_{ij}| < 0$ , ( $j = 1, 2, \dots, n$ ) are satisfied, then  $B$  is a Hurwitz matrix.

First let us write matrix  $\mathbf{A}^k$  in details as

$$\mathbf{A}^k = [a_{ij}] = \begin{bmatrix} w_{11}^k - 1 & w_{12}^k & \cdots & w_{1n}^k \\ w_{21}^k & w_{22}^k - 1 & \cdots & w_{2n}^k \\ \vdots & \vdots & \cdots & \vdots \\ \vdots & \vdots & \cdots & \vdots \\ w_{n1}^k & w_{n2}^k & \cdots & w_{nn}^k - 1 \end{bmatrix}_{n \times n}. \quad (34)$$

Based on Theorem 2 we can check our matrix  $\mathbf{A}^k$ . We clearly see that the condition C1 is easily satisfied because all diagonal elements  $w_{ii}^k$  of the matrix  $\mathbf{w}^k$  satisfy  $0 < w_{ii}^k < 1$  (see property P2 of the matrix  $\mathbf{w}^k$ ). Therefore, all diagonal elements of the matrix  $\mathbf{A}^k$  satisfy  $a_{ii} = w_{ii}^k - 1 < 0$ .

For the condition C2, since the sum of all elements in each row of the matrix  $\mathbf{w}^k$  equals to one (see property P3 of the matrix  $\mathbf{w}^k$ ), we can easily find the constants  $c_i$  to let  $c_j a_{jj} + \sum_{i=1, i \neq j}^n |c_i| |a_{ij}| < 0$ . Therefore, we can conclude that  $\mathbf{A}^k$  is a Hurwitz matrix, or the proposed system (33) is stable.

As one example we can show that  $\mathbf{A}^k$  is a Hurwitz matrix by checking the roots of the characteristic equation (35) in the case of  $2 \times 2$  dimension of the matrix  $(\lambda + 1)\mathbf{I} - \mathbf{w}^k$ .

We have the following characteristic equation for the system (33) as:

$$\det(\lambda\mathbf{I} - \mathbf{A}) = \det(\lambda\mathbf{I} - \mathbf{w}^k + \mathbf{I}) = \det(\mathbf{H}) = 0 \quad (35)$$

here  $\mathbf{H} = (\lambda + 1)\mathbf{I} - \mathbf{w}^k$ , or we have

$$\mathbf{H} = \begin{bmatrix} \lambda + 1 - w_{11}^k & -w_{12}^k & \dots & -w_{1n}^k \\ -w_{21}^k & \lambda + 1 - w_{22}^k & \dots & -w_{2n}^k \\ \vdots & \vdots & \dots & \vdots \\ \vdots & \vdots & \dots & \vdots \\ -w_{n1}^k & -w_{n2}^k & \dots & \lambda + 1 - w_{nn}^k \end{bmatrix}. \quad (36)$$

For the case of  $2 \times 2$  dimension of the matrix  $\mathbf{H}$  we have

$$\begin{aligned} \det(\mathbf{H}) &= \lambda^2 + \lambda(2 - w_{11}^k - w_{22}^k) + 1 - w_{11}^k \\ &\quad - w_{22}^k + w_{11}^k w_{22}^k - w_{21}^k w_{12}^k \\ &= 0. \end{aligned} \quad (37)$$

From the the property P3 of the matrix  $\mathbf{w}^k$  we have  $w_{12}^k = 1 - w_{11}^k$  and  $w_{21}^k = 1 - w_{22}^k$ . Plug these  $w_{12}^k$  and  $w_{21}^k$  into (37) we obtain

$$\det(\mathbf{H}) = \lambda[\lambda + (2 - w_{11}^k - w_{22}^k)] = 0. \quad (38)$$

Equation (38) has two roots  $\lambda_1 = 0$ , and  $\lambda_2 = -2 + w_{11}^k + w_{22}^k < 0$  since  $0 < w_{11}^k < 1$  and  $0 < w_{22}^k < 1$ . This completes the proof for Theorem 1. ■

## REFERENCES

- [1] I. I. Hussein, "A Kalman filter-based control strategy for dynamic coverage control," in *Proc. ACC*, New York, NY, USA, 2007, pp. 3271–3276.
- [2] J. Cortes, S. Martinez, T. Karatas, and F. Bullo, "Coverage control for mobile sensing networks," *IEEE Trans. Robot. Autom.*, vol. 20, no. 2, pp. 243–255, Apr. 2004.
- [3] F. Zhang, D. M. Fratantoni, D. Paley, J. Lund, and N. E. Leonard, "Control of coordinated patterns for ocean sampling," *Int. J. Control*, vol. 80, no. 7, pp. 1186–1199, 2007.
- [4] F. Zhang and N. E. Leonard, "Cooperative filters and control for cooperative exploration," *IEEE Trans. Autom. Control*, vol. 55, no. 3, pp. 650–663, Mar. 2010.
- [5] DCSL. (2006). *DOD/ONR MURI: Adaptive Sampling and Prediction Project* [Online]. Available: <http://www.princeton.edu/~dcsl/asap/>
- [6] J. Choi, S. Oh, and R. Horowitz, "Distributed learning and cooperative control for multi-agent systems," *Automatica*, vol. 45, no. 12, pp. 2802–2814, 2009.
- [7] W. Burgard, M. Moors, C. Stachniss, and F. Schneider, "Coordinated multirobot exploration," *IEEE Trans. Robot.*, vol. 21, no. 3, pp. 376–386, Jun. 2005.
- [8] D. Fox *et al.*, "Distributed multirobot exploration and mapping," *Proc. IEEE*, vol. 94, no. 7, pp. 1325–1339, Jul. 2006.
- [9] A. Dhariwal, G. S. Sukhatme, and A. A. G. Requicha, "Bacterium inspired robots for environmental monitoring," in *Proc. IEEE ICRA*, 2004, pp. 1436–1443.
- [10] M. Bryson, A. Reid, F. Ramos, and S. Sukkarieh, "Airborne vision-based mapping and classification of large farmland environments," *J. Field Robot.*, vol. 27, no. 5, pp. 632–655, 2010.
- [11] A. Guez and J. Pineau, "Multi-tasking SLAM," in *Proc. IEEE ICRA*, Anchorage, AK, USA, 2010, pp. 377–384.
- [12] M. Jadaliha and J. Choi, "Environmental monitoring using autonomous aquatic robots: Sampling algorithms and experiments," *IEEE Trans. Control Syst. Tech.*, vol. 21, no. 3, pp. 899–905, May 2013.
- [13] A. Lilienthal *et al.*, "Gas source declaration with a mobile robot," in *Proc. IEEE ICRA*, 2004, pp. 1430–1435.
- [14] D. V. Zarzhitsky, D. F. Spears, and D. R. Thayer, "Experimental studies of swarm robotic chemical plume tracing using computational fluid dynamics simulations," *Int. J. Intell. Comput. Cybern.*, vol. 3, no. 4, pp. 1–44, 2010.
- [15] GLERL. (2009). *Center of Excellence for Great Lakes, Harmful Algal Bloom Event Response* [Online]. Available: <http://www.glerl.noaa.gov/res/centers/habs/habs.html>
- [16] National Oceanic and Atmospheric Administration. (2013). *Harmful Algal Blooms Observing System (HABSOS)* [Online]. Available: <http://habsos.noaa.gov/>
- [17] H. M. La and W. Sheng, "Distributed sensor fusion for scalar field mapping using mobile sensor networks," *IEEE Trans. Cybern.*, vol. 43, no. 2, pp. 766–778, Apr. 2012.
- [18] H. M. La and W. Sheng, "Cooperative sensing in mobile sensor networks based on distributed consensus," in *Proc. SPIE*, San Diego, CA, USA, 2011.
- [19] K. M. Lynch, P. Yang, and R. A. Freeman, "Decentralized environmental modeling by mobile sensor networks," *IEEE Trans. Robot.*, vol. 24, no. 3, pp. 710–724, Jun. 2008.
- [20] T. H. Chung, V. Gupta, J. W. Burdick, and R. M. Murray, "On a decentralized active sensing strategy using mobile sensor platforms in a network," in *Proc. 43th IEEE CDC*, 2004, pp. 1914–1919.
- [21] T. H. Chung, J. W. Burdick, and R. M. Murray, "Decentralized motion control of mobile sensing agents in a network," in *Proc. 44th IEEE CDC*, 2005.
- [22] P. Yang, R. A. Freeman, and K. M. Lynch, "Distributed cooperative active sensing using consensus filters," in *Proc. IEEE Int. Conf. Robot. Autom.*, Rome, Italy, 2007, pp. 405–410.
- [23] J. Cortes, "Distributed Kriged Kalman filter for spatial estimation," *IEEE Trans. Autom. Control*, vol. 54, no. 12, pp. 2816–2827, Dec. 2009.
- [24] T. B. Curtin, J. G. Bellingham, J. Catipovic, and D. Webb, "Autonomous oceanographic sampling networks," *Oceanography*, vol. 6, no. 3, pp. 86–94, 1993.
- [25] R. A. Cortez and H. G. Tanner, "Radiation mapping using multiple robots," in *Proc. 2nd Int. Joint Topical Meeting Emergency Preparedness Response Robotic Remote Syst.*, 2008.
- [26] H. G. Tanner, R. A. Cortez, and R. Lumia, "Distributed robotic radiation mapping," in *Proc. 11th Experiment. Robot.*, Berlin, Germany, 2009, pp. 147–156.
- [27] C. Zhang, D. Arnold, N. Ghods, A. Siranosian, and M. Krstic, "Source seeking with nonholonomic unicycle without position measurement Part 1: Tuning of forward velocity," in *Proc. IEEE CDC*, San Diego, CA, USA, 2006, pp. 3040–3045.
- [28] S. Pang and J. A. Farrell, "Chemical plume source localization," *IEEE Trans. Syst., Man, Cybern.*, vol. 36, no. 5, pp. 1068–1080, Oct. 2006.
- [29] A. R. Mesquita, J. P. Hespanha, and K. Astrom, "ptimotaxis: A stochastic multi-agent on site optimization procedure," in *Proc. 11th Int. Conf. Hybrid Syst. Comput. Control*, 2008.
- [30] C. G. Mayhew, R. G. Sanfelice, and A. R. Teel, "Robust source-seeking hybrid controllers for autonomous vehicles," in *Proc. ACC*, New York, NY, USA, 2007, pp. 1185–1190.
- [31] C. Stachniss, C. Plagemann, A. J. Lilienthal, and W. Burgard, "Gas distribution modeling using sparse Gaussian process mixture models," in *Proc. Robot. Sci. Syst.*, 2008.
- [32] A. J. Lilienthal, M. Reggente, M. Trincavelli, J. L. Blanco, and J. Gonzalez, "A statistical approach to gas distribution modelling with mobile robots—The Kernel DM+V algorithm," in *Proc. IEEE Int. Conf. IROS*, St. Louis, MO, USA, 2009, pp. 570–576.
- [33] S. Martinez and F. Bullo, "Optimal sensor placement and motion coordination for target tracking," *Automatica*, vol. 42, no. 4, pp. 661–668, Apr. 2006.
- [34] H. M. La, W. Sheng, and J. Chen, "Cooperative and active sensing in mobile sensor networks for scalar field mapping," in *Proc. IEEE CASE*, Madison, WI, USA, 2013, pp. 831–836.

- [35] A. Krause, A. Singh, and C. Guestrin, "Near-optimal sensor placements in gaussian processes: Theory, efficient algorithms and empirical studies," *J. Mach. Learn. Res.*, vol. 9, pp. 235–284, Jan. 2008.
- [36] R. Graham and J. Cortes, "Spatial statistics and distributed estimation by robotic sensor networks," in *Proc. ACC*, Baltimore, MD, USA, 2010, pp. 2422–2427.
- [37] Z. Feng, S. Jaewon, and R. James, "Information-driven dynamic sensor collaboration for target tracking," *IEEE Signal Process. Mag.*, vol. 19, no. 2, pp. 61–72, Mar. 2002.
- [38] J. Spletzer and C. Taylor, "Dynamic sensor planning and control for optimally tracking targets," *Int. J. Robot. Res.*, vol. 22, pp. 7–20, Jan. 2003.
- [39] H. M. La and W. Sheng, "Flocking control of a mobile sensor network to track and observe a moving target," in *Proc. IEEE ICRA*, Kobe, Japan, 2009, pp. 3129–3134.
- [40] H. M. La and W. Sheng, "Adaptive flocking control for dynamic target tracking in a mobile sensor network," in *Proc. IEEE/RSJ Int. Conf. IROS*, St. Louis, MO, USA, 2009, pp. 4843–4848.
- [41] H. M. La and W. Sheng, "Flocking control of multiple agents in noisy environments," in *Proc. IEEE ICRA*, Anchorage, AK, USA, 2010, pp. 4964–4969.
- [42] L. Xiao, S. Boy, and S. Lall, "A scheme for robust distributed sensor fusion based on average consensus," in *Proc. Int. Conf. IPSN*, Los Angeles, CA, USA, 2005, pp. 63–70.
- [43] R. Olfati-Saber, J. Alex Fax, and R. M. Murray, "Consensus and cooperative in networked multi-agent systems," *Proc. IEEE*, vol. 95, no. 1, pp. 215–233, Jan. 2007.
- [44] S. Kar and J. M. F. Moura, "Distributed consensus algorithms in sensor networks with imperfect communication: Link failures and channel noise," *IEEE Trans. Signal Process.*, vol. 57, no. 1, pp. 355–369, Jan. 2009.
- [45] R. Olfati-Saber, "Flocking for multi-agent dynamic systems: Algorithms and theory," *IEEE Trans. Autom. Control*, vol. 51, no. 3, pp. 401–420, Mar. 2006.
- [46] H. M. La and W. Sheng, "Dynamic targets tracking and observing in a mobile sensor network," *Robot. Autonom. Syst.*, vol. 60, no. 7, pp. 996–1009, Jul. 2012.
- [47] H. K. Khalil, *Nonlinear Systems*, 3rd ed. Upper Saddle River, NJ, USA: Prentice Hall, 2002.
- [48] X. Liao, L. Wang, and P. Yu, *Stability of Dynamical Systems*, 1st ed. Amsterdam, The Netherlands: Elsevier, 2007.



**Hung M. La** (M'09) received the B.S. and M.S. degrees in electrical engineering from Thai Nguyen University of Technology, Thai Nguyen, Vietnam, in 2001 and 2003, respectively, and the Ph.D. degree in electrical and computer engineering from Oklahoma State University, Stillwater, OK, USA, in 2011.

He is an Assistant Professor at the Department of Computer Science and Engineering, University of Nevada, Reno, NV, USA. During 2001–2007, he was a Lecturer at the Department of Electrical Engineering, Thai Nguyen University of Technology.

From 2011 to 2014, he was a Post Doctor and then a Research Associate at the Center for Advanced Infrastructure and Transportation (CAIT), Rutgers University, Piscataway, NJ, USA. He was a key team member of the CAIT team that developed the Robotics Assisted Bridge Inspection Tool (RABIT) for the Federal Highway Administration (FHWA). He has been actively involved in research projects with the FHWA, National Institute of Standards and Technology (NIST), U.S. Department of Transportation (DoT), Department of Defense (DoD), and National Science Foundation (NSF). He has authored over 30 papers published in major journals, book chapters and international conference proceedings. His current research interests include mobile robotic systems, mobile sensor networks, cooperative control, learning and sensing, and intelligent transportation systems.

Dr. La and his team received the 2014 American Society of Civil Engineers Charles Pankow Award for Innovation for the Robotics Assisted Bridge Inspection Tool (RABIT). He is the recipient of two best paper awards and a best presentation award in international conferences.



**Weihua Sheng** (M'02–SM'08) received the B.S. and M.S. degrees in electrical engineering from Zhejiang University, Zhejiang, China, in 1994 and 1997, respectively, and the Ph.D. degree in electrical and computer engineering from Michigan State University, East Lansing, MI, USA, in May 2002.

He is an Associate Professor at the School of Electrical and Computer Engineering, Oklahoma State University, Stillwater, OK, USA. During 1997–1998, he was a Research Engineer at the Research and Development Center at Huawei Technologies Corporation, Shenzhen, China. From 2002 to 2006, he taught in the Electrical and Computer Engineering Department, Kettering University, Flint, MI, USA (formerly General Motor Institute). He holds one U.S. patent and has authored over 130 papers in major journals and international conferences. His current research interests include wearable computing, mobile robotics, human robot interaction, and intelligent transportation systems.

Dr. Sheng has participated in organizing various IEEE international conferences and workshops in the area of intelligent robots and systems. He is currently an Associate Editor for the IEEE TRANSACTIONS ON AUTOMATION SCIENCE AND ENGINEERING. He is the recipient of six best paper awards in international conferences. His research was supported by NSF, DoD, DEPSCoR, and DoT.



**Jiming Chen** (M'08–SM'11) received the B.Sc. and Ph.D. degrees in control science and engineering from Zhejiang University, Zhejiang, China, in 2000 and 2005, respectively.

He was a Visiting Researcher at INRIA, Valbonne, France, in 2006, at the National University of Singapore, Singapore, in 2007, and at the University of Waterloo, Waterloo, ON, Canada, from 2008 to 2010. Currently, he is a Full Professor with the Department of Control Science and Engineering, and the Coordinator of Group of

Networked Sensing and Control in the State Key Laboratory of Industrial Control Technology, Vice Director of Institute of Industrial Process Control at Zhejiang University.

Dr. Chen currently serves as an Associate Editor for several international journals including the IEEE TRANSACTIONS ON PARALLEL AND DISTRIBUTED SYSTEMS, IEEE TRANSACTIONS ON INDUSTRIAL ELECTRONICS, IEEE NETWORKS, and the IEEE TRANSACTIONS ON CONTROL OF NETWORK SYSTEMS. He was a Guest Editor for the IEEE TRANSACTIONS ON AUTOMATIC CONTROL, *Computer Communication* (Elsevier), *Wireless Communication and Mobile Computer* (Wiley), and *Journal of Network and Computer Applications* (Elsevier). He also served/serves as an Ad hoc and Sensor Network Symposium Co-Chair, IEEE Globecom 2011; General Symposia Co-Chair of ACM IWCMC 2009 and ACM IWCMC 2010, WiCON 2010 MAC track Co-Chair, IEEE MASS 2011 Publicity Co-Chair, IEEE DCOSS 2011 Publicity Co-Chair, IEEE ICDCS 2012 Publicity Co-Chair, IEEE ICC 2012 Communications QoS and Reliability Symposium Co-Chair, IEEE SmartGridComm The Whole Picture Symposium Co-Chair, IEEE MASS 2013 Local Chair, Wireless Networking and Applications Symposium Co-Chair, IEEE ICC 2013, Ad hoc and Sensor Network Symposium Co-Chair, IEEE ICC 2014, and TPC member for IEEE ICDCS 2010 and 2012–2014; IEEE MASS 2010, 2011, and 2013; IEEE SECON 2011 and 2012; and IEEE INFOCOM 2011–2014.